



Published in final edited form as:

*Kidney Int Rep.* 2017 January ; 2(1): 36–43. doi:10.1016/j.ekir.2016.09.003.

## Evaluation of Renal Blood Flow in Chronic Kidney Disease Using Arterial Spin Labeling Perfusion Magnetic Resonance Imaging

Lu-Ping Li, Ph.D.<sup>1</sup>, Huan Tan, Ph.D.<sup>1</sup>, Jon M. Thacker, M.S.<sup>2</sup>, Wei Li, M.D.<sup>1</sup>, Ying Zhou, Ph.D.<sup>3</sup>, Orly Kohn, M.D.<sup>5</sup>, Stuart M. Sprague, D.O.<sup>4,5</sup>, and Pottumarthi V. Prasad, Ph.D.<sup>1</sup>

<sup>1</sup>Center for Advanced Imaging, NorthShore University HealthSystem, Evanston, IL

<sup>2</sup>Department of Biomedical Engineering, Northwestern University, Evanston, IL

<sup>3</sup>Center for Biomedical Research & Informatics, NorthShore University HealthSystem, Evanston, IL

<sup>4</sup>Department of Nephrology, NorthShore University HealthSystem, Evanston, IL

<sup>5</sup>Department of Nephrology, University of Chicago, Chicago, IL

### Abstract

**Introduction**—Chronic kidney disease (CKD) is known to be associated with reduced renal blood flow. However, data to-date in humans is limited.

**Methods**—In this study, non-invasive arterial spin labeling (ASL) MRI data was acquired in 33 patients with diabetes and stage-3 CKD, and 30 healthy controls.

**Results**—A significantly lower renal blood flow both in cortex ( $108.4 \pm 36.4$  vs.  $207.3 \pm 41.8$ ;  $p < 0.001$ ,  $d = 2.52$ ) and medulla ( $23.2 \pm 8.9$  vs.  $42.6 \pm 15.8$ ;  $p < 0.001$ ,  $d = 1.5$ ) was observed. Both cortical ( $\rho = 0.67$ ,  $p < 0.001$ ) and medullary ( $\rho = 0.62$ ,  $p < 0.001$ ) blood flow were correlated with eGFR, and cortical blood flow was found to be confounded by age and BMI. However, in a subset of subjects that were matched for age and BMI ( $n = 6$ ), the differences between CKD and control subjects remained significant both in cortex ( $107.4 \pm 42.8$  vs.  $187.51 \pm 20.44$ ;  $p = 0.002$ ) and medulla ( $15.43 \pm 8.43$  vs.  $39.18 \pm 11.13$ ;  $p = 0.002$ ). A threshold value to separate healthy and CKD was estimated to be  $Cor\_BF = 142.9$  and  $Med\_BF = 24.1$ .

**Conclusion**—These results support the use of ASL in the evaluation of renal blood flow in patients with moderate level of CKD. Whether these measurements can identify subjects at risk of progressive CKD requires further longitudinal follow-up.

### Keywords

chronic kidney disease; renal blood flow; MRI; perfusion; arterial spin labeling; eGFR

---

**Address for correspondence:** Pottumarthi V. Prasad, Ph.D., Department of Radiology, NorthShore University HealthSystem, 2650 Ridge Avenue, Evanston, IL 60035, Tel: 847-570-1349, Fax: 847-570-2942, pprasad@northshore.org.

**Publisher's Disclaimer:** This is a PDF file of an unedited manuscript that has been accepted for publication. As a service to our customers we are providing this early version of the manuscript. The manuscript will undergo copyediting, typesetting, and review of the resulting proof before it is published in its final citable form. Please note that during the production process errors may be discovered which could affect the content, and all legal disclaimers that apply to the journal pertain.

**FINANCIAL DISCLOSURE:** Authors have no financial conflict of interest to declare.

## INTRODUCTION

Recent advances in understanding the pathophysiology of chronic kidney disease (CKD) suggest that the pathogenic mechanisms causing *progressive* renal destruction converge on a common tubulo-interstitial pathway characterized by tubular atrophy and hypoxia, peritubular capillary injury, and interstitial fibrosis, finally leading to irreversible scarring<sup>1, 2</sup>. Prior studies have evaluated the use of blood oxygenation level dependent (BOLD) and diffusion MRI to monitor differences in relative levels of hypoxia and interstitial fibrosis in patients with CKD<sup>3, 4</sup>. The key advantage of these two methods is that they are both endogenous contrast mechanisms and require no administration of exogenous contrast media which are contraindicated in subjects with compromised renal function<sup>5</sup>. Ability to include an endogenous method to evaluate renal perfusion would be of great interest in developing a comprehensive functional protocol to understand the natural progression of CKD. Currently, there is not much data on renal blood flow or perfusion in subjects with CKD.

Arterial spin labeling (ASL) MRI uses endogenous water as a tracer and is widely used in the brain<sup>6</sup>. Even though feasibility has been demonstrated in the kidneys<sup>7, 8</sup>, a key challenge for ASL MRI is the inherently limited signal to noise ratio (SNR) necessitating repeated measurements to allow data averaging<sup>9</sup>. This is a major hurdle in the abdomen since breath-holding limits the number of averages that can be performed. While feasibility of renal perfusion MRI with ASL has been demonstrated using breath-hold acquisitions in healthy subjects<sup>7</sup>, it is more challenging in patients with compromised renal perfusion. Coached breathing<sup>10-12</sup> or navigator gated acquisitions<sup>13</sup> have been used. Navigator gating involves additional data acquisition to estimate the motion which can be used to decide whether to accept or reject the measurement. In prospective gating, this decision is made in real-time. In retrospective gating, a fixed number of data acquisitions are made and accept or reject decisions are made retrospectively. In this study, we have evaluated renal perfusion using a retrospectively navigator gated ASL MRI sequence<sup>13</sup> in a sufficiently large number of subjects with chronic kidney disease and healthy controls with no known renal disease.

## MATERIALS AND METHODS

### Subjects

All procedures were performed with the approval from the institutional review board and written subject consent prior to enrollment. MRI data was acquired in a group of diabetics with stage 3 CKD (n=33) and healthy subjects (n=30) with no known renal disease. Subjects were instructed not to take NSAIDs for 3 days and ACEi/ARB 1 day prior to MRI. Both groups were instructed to fast after midnight on the day of the MRI and take half the dose of insulin if applicable. Blood was drawn for estimated glomerular filtration rate (eGFR) calculation either on the day of the scan for healthy subjects or during the screening visit prior to MRI scan for patients. The Chronic Kidney Disease Epidemiology Collaboration (CKD-EPI) equation was used for eGFR calculation<sup>29</sup>. Twenty four hour urine samples were collected within a few days after MRI scan in most of the patients with CKD (28/33) for analysis of urine creatinine and protein excretion.

Because data was acquired in the fasted status, in eight of the healthy subjects ( $30.6 \pm 11.1$  years), we also evaluated any potential effect of hydration on ASL derived perfusion measurement on a separate day. For these studies, subjects followed the same preparation as above. Urine specific gravity was used to document the subject's hydration status. Urine samples were acquired prior to the baseline scan, and one following each acquisition after water-loading. Following the ASL baseline scan, subjects drank water based on their body weight (20 ml / kg) within 15 minutes. Post water-loading, ASL MRI data was acquired two times.

### MRI acquisition methods

All the studies were performed on a 3.0T MRI system (MAGNETOM Verio, Siemens Healthcare, Erlangen, Germany) equipped with high performance gradient coils (45 mT/m maximum gradient strength, 200 mT/m/ms slew rate). The body coil was used as the transmitter, and the combination of spine and body array coils was used as the receiver. Subjects were positioned feet first and supine.

The renal perfusion measurement was performed using the 2D navigator-gated FAIR True-FISP sequence<sup>13</sup>. A 10.24 ms adiabatic frequency offset corrected inversion (FOCI) pulse ( $\mu=6$ ,  $\beta=1078$ ) was used for selective inversion<sup>30</sup>. The scan prescription included: 1) Defining the imaging slice (thickness = 8 mm) position in an oblique coronal orientation to match the longitudinal axis of both kidneys; 2). Positioning a slice selective inversion band (thickness = 30 mm) over the imaging slice with care taken to avoid intersection with major arteries; and 3). Choosing the slice position for the navigator in the coronal plane. To allow sufficient labeled blood to perfuse into the tissue, an inversion pulse delay time (TI) of 1.5 s for healthy or 2.0 s for patients was used<sup>13</sup>. The imaging readout used a true FISP sequence (TR/TE=4.0/2.02 ms; FA=60°; FOV=360–400 mm; matrix= 128×128; BW=651 Hz/pixel). The 2D navigator acquisition was performed immediately following the imaging readout using a FLASH readout (TR/TE=2.2/1.2 ms; FA=5°; FOV=400×400 mm<sup>2</sup>; matrix= 96×96; BW=1000 Hz/pixel; GRAPPA factor=2).

The acquisition efficiency of this 2D navigator in a previous study was about 35% (26% – 39%) in patients and 50% (35% – 65%) in healthy subjects depending on the respiratory pattern<sup>13</sup>. To maintain protocol consistency, we took a conservative approach and acquired 50 control/label pairs of perfusion weighted images (PWI) with a total scan time of 5 min in healthy subjects and 100 control/label pairs of PWI with a total scan time of 10 min during free-breathing in subjects with CKD. A proton density weighted (M0) image was acquired using an identical True-FISP readout with a pulse repetition time of 10 s and no inversion pulse.

### MRI analysis methods

ASL maps were reconstructed using a MATLAB (MathWorks, Natick, MA) based custom suite of software<sup>13</sup>. Navigator data was used to estimate the translational motion in the coronal plane. Only images where the diaphragm position was within the acceptance window (8 mm width) were selected for the perfusion calculation. This processing scheme leads to a variation in the final number of selected control and label images for each subject.

Selected images were further realigned using the FMRIB's Linear Image Registration Tool (FLIRT, FMRIB, Oxford, United Kingdom)<sup>31</sup>. The first image of each sequence was used as the reference and the remaining images were aligned to it. Control and label images were then separately averaged to yield a single control image and a single label image. The final perfusion weighted image was computed by subtracting the averaged control from the averaged label image. Quantitative renal blood flow was calculated pixel-by-pixel using a single compartment model<sup>32</sup>:

$$f = \frac{\lambda}{2\alpha T_1} \frac{\Delta M(TI)}{M_0} \exp\left(\frac{-TI}{T_1}\right)$$

where  $f$  is the perfusion rate (in the unit of mL/100 g/min),  $\lambda$  is the blood–tissue–water partition coefficient, which was assumed to be 80 mL/100 g<sup>33</sup>,  $\alpha$  is the inversion efficiency which was assumed to be 0.95,  $M(TI)$  is the perfusion weighted image, and  $M_0$  is the equilibrium magnetization of the tissue (proton density). The  $T_1$  value of 1.15 s for renal cortex<sup>34</sup> is assumed to be the  $T_1$  of the blood.

Regions of interest (ROI) were manually defined in the cortex (Cor\_BF) and medulla (Med\_BF) on ASL maps using a custom image processing toolbox written in Python (Python Software Foundation)<sup>35, 36</sup>. ROIs were defined in the cortex and medulla for both the left and right kidneys. Tumors and cysts were excluded from the ROIs. Cortical ROI was defined as one large ROI (>500 voxels) encompassing the vast majority of the cortex. Medullary ROIs were drawn using a freehand tool and typically consisted of less than 100 voxels. After all the ROIs were defined for both kidneys in each subject, the mean value of each region was computed to get one representative value per subject per region (cortex and medulla).

### Statistical methods

Two-sample T-test or Wilcoxon rank sum test (if normality in distribution was not observed) was used to compare the various MRI derived parameters along with age and eGFR between the CKD and control groups. We included Cohen's  $d$  value as the measure of the magnitude of difference between groups. Cohen's  $d$  represents the effect size and in this study we recognize three levels: small, medium and large. These levels correspond to  $d$  values greater than or equal to 0.2, 0.5 and 0.8 respectively<sup>37</sup>.

Spearman correlation coefficients were calculated among the following variables: Cor\_BF, Med\_BF, eGFR, age and BMI.  $p$  values are reported for all statistical tests. Linear regression was used to explore the pair-wise relationship between Cor\_BF, Med\_BF and eGFR. Multiple linear regressions were used to explore the pair-wise relationship accounting for any potential confounding effect of age, gender, race or BMI where appropriate. The confounder was retained in the model if it changed the regression coefficient of eGFR more than 15%. Parameter estimate, standard error (SE) and  $p$  values were reported for the regression analyses.

Aside from the regression analysis, the confounding effects (if any) in the above mentioned analysis were removed by conducting a 1:1 age-, gender-, race- or BMI- matching between

CKD and control groups. The propensity score matching method used a greedy 8-to-1 matching algorithm for identifying matched pairs.

The Cor\_BF and Med\_BF readings from two groups were used to assess if ASL measurement can be used to discriminate CKD from healthy subjects. The optimal thresholds for Cor\_BF and Med\_BF were determined by conducting a Receiver Operating Characteristic (ROC) utilizing each measure (Cor\_BF and Med\_BF) alone as a continuous variable to distinguish abnormal perfusion in CKD from normal subjects. Areas Under the Curve (AUCs) were estimated with a 95% confidence interval. Sensitivity and specificity for the optimal threshold for each measure were determined by the Youden Index.

Repeated-measure analysis of variance was used to compare the changes from baseline for cor\_BF and specific gravity for water-loading results. Multiple comparisons were adjusted.

All of the statistical analyses were carried out in SAS 9.3 (SAS, Cary, NC, USA), and  $p$  value  $< 0.05$  was regarded as statistically significant.

## RESULTS

Thirty three subjects with CKD patients and 30 control subjects participated in our study (Table 1-1). The median eGFR and 24 hour urine protein excretion in patients was 46.7 ml/min/1.73 m<sup>2</sup> and 0.18 gm respectively (Table 1-2). However, most of the subjects with CKD were taking angiotensin converting enzyme inhibitors (ACEi) or angiotensin receptor blockers (ARBs). There were significantly higher proportion of female patients in CKD group than the healthy controls (54.6% vs. 20%,  $p = 0.0048$ ). Both groups had similar proportion of African American to Caucasian subjects.

Figure 1 shows representative renal perfusion maps from a healthy subject and one with CKD. The color bar shows the blood flow in units of ml/min/100g. One can appreciate the lower renal blood flow in subject with CKD compared to the healthy subject.

Table 2 is the summary of variables in this study based on groups. All variables, age, eGFR, BMI, cortical blood flow (Cor\_BF), and medullary blood flow (Med\_BF) were significantly different between CKD and controls ( $p$  values  $< 0.0001$   $d$  values  $> 1.4$  (1.4 to 3.19)).

Additionally, there was no difference between left and right kidneys in both CKD and control groups (data not shown).

Table 3 shows all pair-wise correlation among variables age, eGFR, Cor\_BF, Med\_BF and BMI. Since age, Cor\_BF and Med\_BF were correlated with eGFR, a regression analysis was conducted to test for potential confounding effect of age, race, gender and BMI on the relationship between blood flow with eGFR. Table 4-1 shows the results of the linear regression for both Cor\_BF and Med\_BF against eGFR. Age and BMI were found to be confounding factors by multiple linear regression analysis for Cor\_BF, but not Med\_BF (Table 4\_2) based on changes in the regression coefficient of BF vs. eGFR more than 15%. Table 5 shows the comparison between CKD and healthy controls for age and BMI matched pairs of subjects. All three parameters: eGFR, Cor\_BF, and Med\_BF showed significant

differences between CKD and healthy controls, even though the sample size was small (n=6).

The optimal threshold to separate CKD and healthy for Cor\_BF was estimated to be 142.9 (Youden Index=0.85) and Med\_BF was 24.1 (Youden Index=0.64). The sensitivity and specificity for this threshold was 84.85% and 100.00% for Cor\_BF and 60.61% and 100.00% for Med\_BF. The accuracy was estimated by the AUC (area under the ROC curve). The AUC for Cor\_BF was 0.98, which is rated to be excellent; and for Med\_BF was 0.88, which is rated to be good.

Even though specific gravity showed significant reduction post-water-loading compared to baseline ( $1.00\pm 0.01$  vs.  $1.03\pm 0.0$ ,  $p<0.0001$ ), there was no difference in Cor\_BF ( $208.1\pm 33.4$  vs.  $193.9\pm 26.7$ ,  $p=0.34$ ) and Med\_BF ( $90.6\pm 32.2$  vs.  $91.9\pm 18.4$ ,  $p=0.99$ ) suggesting hydration may not have a significant influence on ASL derived renal perfusion estimates.

## DISCUSSION

Blood flow to the kidneys is thought to be reduced with progression of CKD<sup>2</sup>. The conventional method for measuring renal blood flow is the para-aminohippurate (PAH) clearance method<sup>14</sup>. This is invasive and time consuming and hence only used for research purposes. Contrast enhanced MRI<sup>15</sup> and CT<sup>16</sup> methods can be used to measure renal blood flow, however, they are contraindicated in subjects with CKD<sup>5</sup>. Nuclear medicine based methods are available to estimate renal blood flow<sup>17</sup>, but not widely used in the clinic. Overall, there is very little data available on renal blood flow in subjects with CKD. A recent study used phase contrast MRI to measure blood flow within renal arteries in subjects with CKD and found that the flow was reduced by about 28% while measured-GFR was reduced by 37%<sup>18</sup>.

Prior studies have demonstrated feasibility of acquiring ASL perfusion MRI measurements in the kidneys<sup>7, 8</sup> and preliminary data showed differences between subjects with CKD and healthy controls with small number of subjects<sup>13, 19</sup>. Though only a few studies evaluating ASL MRI measurements have been performed to-date, the technique has been shown to be reproducible<sup>20, 21</sup>. Furthermore, ASL MRI derived perfusion estimates correlated well with PAH measurements and were able to discriminate pharmacologic changes in renal plasma flow<sup>22</sup>. The comparison of ASL technique with microspheres method in an animal model has shown that cortical perfusion measured with ASL correlated with microspheres in the expected physiologic range<sup>23</sup>. In a group of 98 transplant recipients, ASL MRI identified reduced cortical blood flow in subjects with reduced renal function (eGFR  $< 30$  ml/min/1.73 m<sup>2</sup>) compared to those with good to moderate renal function (eGFR  $> 30$  ml/min/1.73 m<sup>2</sup>)<sup>24</sup>.

Consistent with prior reported data, our data shows a significant reduction in cortical and medullary blood flow in subjects with CKD compared to healthy controls in a moderately large number of subjects. We further observed a significant correlation of renal blood flow with eGFR. Cortical blood flow and eGFR reduced by ~50% in CKD compared to controls.

Multiple linear regression analysis found age and BMI to be confounders for cortical blood flow. However, within the age and BMI matched group, the difference in eGFR and renal blood flow between CKD still remained significant.

Proteinuria is a common clinical signature observed in patients with diabetic nephropathy. In our study, the median value of 24 hour urine protein was relatively low (0.175 gm), probably due to the use of ACEi and/or ARBs.

Renal blood flow in CKD patients is about half of that in healthy controls in both renal cortex ( $108.4 \pm 36.4$  vs.  $207.3 \pm 41.8$ ;  $p < 0.001$ ,  $d = 2.52$ ) and medulla ( $23.2 \pm 8.9$  vs.  $42.6 \pm 15.8$ ;  $p < 0.001$ ,  $d = 1.5$ ). Because we performed studies following an overnight fast, we wanted to verify if hydration status has any significant influence on renal blood flow as evaluated by ASL. In a small sub-study, we looked at the effect of water-loading in fasted healthy subjects on ASL measurements. While the urine specific gravity changed significantly post-water-loading, the renal perfusion estimates did not change. This suggests that ASL MRI based perfusion estimates may not be influenced by hydration status within normal limits.

There are a few limitations in this study. The control group was not age, sex and BMI matched with the CKD group. Even though age and BMI were found to be confounding factors in the relationship between cortical blood flow and eGFR, when identifying a sub-group with matched age and BMI, both cortical and medullary blood flow were significantly lower in subjects with CKD compared to the control group. The ASL MRI protocol used here required 5 to 10 minutes for data acquisition. Even though these are during free breathing, it could be considered to be long especially for a single slice acquisition. For this preliminary study, we were conservative and acquired more data than necessary. In a small number of subjects with CKD ( $n = 6$ ), data using only half the number of acquired images yielded comparable perfusion estimates (data not shown). These preliminary data could be used to optimize the total acquisition time for future use. Absolute quantification of renal blood flow with the present implementation of ASL has not yet been validated, *e.g.* against microspheres. The current values for cortical perfusion ( $\sim 200$  ml/min/100gm) are lower than our own previous report ( $\sim 260$  ml/min/100gm). The key difference between these two studies is that the subjects in the current study were fasted before the scan. In fact, that was the motivation to study the potential effects of water-loading on renal perfusion. We may need future studies to verify the effects of fasting. Even though a previous study has validated ASL estimated cortical perfusion against microspheres<sup>23</sup>, no such validation is available for medullary blood flow estimates. ASL is inherently limited in sensitivity to low flow. However, the primary interest in routine use demands precision rather than accuracy. Recent report suggests high degree of reproducibility of renal ASL MRI when repeated after two weeks<sup>20</sup>. In this study, we used longer TI for patients assuming slower circulation compared to controls<sup>13, 27</sup>. While not ideal, this should not unduly influence the estimated flow since the quantitation takes TI in to account. In a healthy volunteer, the flow estimates were relatively stable for a range of TI values between 1 and 2s ( $146.4 \pm 15.9$  ml/min/100gm). The values for TI outside this range were considerably lower. Future studies may have to include multiple TIs to estimate both average transit times and transit time corrected blood flow estimates, as suggested by a recent report<sup>27</sup>.

In conclusion, ASL derived renal perfusion values were significantly lower in the subjects with CKD and correlated with eGFR. Both cortical blood flow and eGFR were reduced about 50% in the CKD group compared to controls. Overall, the data presented here, along with other recent studies support the feasibility of using ASL perfusion MRI in the evaluation of CKD to identify early markers of progression. The significant and large difference between CKD and healthy makes this ASL technique a potential tool to document the change in perfusion in longitudinal studies. Combined with BOLD MRI to evaluate relative renal hypoxia and diffusion MRI to evaluate fibrosis<sup>3, 4</sup>, a comprehensive and non-invasive suite of tools may now be available for evaluating the chronic hypoxia hypothesis<sup>2</sup>. The differences observed here between CKD and control groups are probably smaller compared to those with progressive CKD and controls, since only a third of the subjects with diabetes may show progressive decline in renal function<sup>28</sup>.

## Supplementary Material

Refer to Web version on PubMed Central for supplementary material.

## ACKNOWLEDGEMENTS

The work was supported in part by a grant funded by National Institutes of Health (DK079080 and DK093793). We want to thank Ms. Shoshana Fettman and Claire Feczko for their technical assistance during the study.

## REFERENCES

1. Fine LG, Norman JT. Chronic hypoxia as a mechanism of progression of chronic kidney diseases: from hypothesis to novel therapeutics. *Kidney Int.* 2008; 74:867–72. doi:ki2008350 [pii] 10.1038/ki.2008.350. [PubMed: 18633339]
2. Fine LG, Orphanides C, Norman JT. Progressive renal disease: the chronic hypoxia hypothesis. *Kidney Int Suppl.* 1998; 65:S74–8. [PubMed: 9551436]
3. Inoue T, Kozawa E, Okada H, et al. Noninvasive evaluation of kidney hypoxia and fibrosis using magnetic resonance imaging. *J Am Soc Nephrol.* 2011; 22:1429–34. doi:10.1681/ASN.2010111143. [PubMed: 21757771]
4. Prasad PV, Thacker J, Li LP, et al. Multi-Parametric Evaluation of Chronic Kidney Disease by MRI: A Preliminary Cross-Sectional Study. *PLoS One.* 2015; 10:e0139661. doi:10.1371/journal.pone.0139661. [PubMed: 26430736]
5. Wagner LA, Tata AL, Fink JC. Patient safety issues in CKD: core curriculum 2015. *Am J Kidney Dis.* 2015; 66:159–69. doi:10.1053/j.ajkd.2015.02.343. [PubMed: 25987263]
6. Pollock JM, Tan H, Kraft RA, et al. Arterial spin-labeled MR perfusion imaging: clinical applications. *Magn Reson Imaging Clin N Am.* 2009; 17:315–38. doi:10.1016/j.mric.2009.01.008. [PubMed: 19406361]
7. Martirosian P, Klose U, Mader I, et al. FAIR true-FISP perfusion imaging of the kidneys. *Magn Reson Med.* 2004; 51:353–61. doi:10.1002/mrm.10709. [PubMed: 14755661]
8. Prasad PV, Kim D, Kaiser AM, et al. Noninvasive comprehensive characterization of renal artery stenosis by combination of STAR angiography and EPSTAR perfusion imaging. *Magn Reson Med.* 1997; 38:776–87. [PubMed: 9358452]
9. Odudu A, Francis ST, McIntyre CW. MRI for the assessment of organ perfusion in patients with chronic kidney disease. Current opinion in nephrology and hypertension. 2012; 21:64–75. doi: 10.1097/MNH.0b013e328358d582.
10. Artz NS, Sadowski EA, Wentland AL, et al. Arterial spin labeling MRI for assessment of perfusion in native and transplanted kidneys. *Magn Reson Imaging.* 2011; 29:74–82. doi:10.1016/j.mri.2010.07.018. [PubMed: 20850241]



11. Lanzman RS, Robson PM, Sun MR, et al. Arterial spin-labeling MR imaging of renal masses: correlation with histopathologic findings. *Radiology*. 2012; 265:799–808. doi:10.1148/radiol.12112260. [PubMed: 23047841]
12. Niles DJ, Artz NS, Djamali A, et al. Longitudinal Assessment of Renal Perfusion and Oxygenation in Transplant Donor-Recipient Pairs Using Arterial Spin Labeling and Blood Oxygen Level-Dependent Magnetic Resonance Imaging. *Invest Radiol*. 2016; 51:113–20. doi:10.1097/RLI.0000000000000210. [PubMed: 26561047]
13. Tan H, Koktzoglou I, Prasad PV. Renal perfusion imaging with two-dimensional navigator gated arterial spin labeling. *Magn Reson Med*. 2014; 71:570–9. doi:10.1002/mrm.24692. [PubMed: 23447145]
14. Toto RD. Conventional measurement of renal function utilizing serum creatinine, creatinine clearance, inulin and para-aminohippuric acid clearance. *Current opinion in nephrology and hypertension*. 1995; 4:505–9. discussion 3–4. [PubMed: 8591059]
15. Dujardin M, Luybaert R, Vandembroucke F, et al. Combined T1-based perfusion MRI and MR angiography in kidney: first experience in normals and pathology. *Eur J Radiol*. 2009; 69:542–9. doi:10.1016/j.ejrad.2007.11.033. [PubMed: 18164570]
16. Braunagel M, Helck A, Wagner A, et al. Dynamic Contrast-Enhanced Computed Tomography: A New Diagnostic Tool to Assess Renal Perfusion After Ischemia-Reperfusion Injury in Mice: Correlation of Perfusion Deficit to Histopathologic Damage. *Invest Radiol*. 2016; 51:316–22. doi:10.1097/RLI.0000000000000245. [PubMed: 26741893]
17. Akahira H, Shirakawa H, Shimoyama H, et al. Dynamic SPECT evaluation of renal plasma flow using technetium-99m MAG3 in kidney transplant patients. *Journal of nuclear medicine technology*. 1999; 27:32–7. [PubMed: 10322572]
18. Khatir DS, Pedersen M, Jespersen B, et al. Evaluation of Renal Blood Flow and Oxygenation in CKD Using Magnetic Resonance Imaging. *Am J Kidney Dis*. 2015 doi:10.1053/j.ajkd.2014.11.022.
19. Rossi C, Artunc F, Martirosian P, et al. Histogram analysis of renal arterial spin labeling perfusion data reveals differences between volunteers and patients with mild chronic kidney disease. *Invest Radiol*. 2012; 47:490–6. doi:10.1097/RLI.0b013e318257063a. [PubMed: 22766911]
20. Hammon M, Janka R, Siegl C, et al. Reproducibility of Kidney Perfusion Measurements With Arterial Spin Labeling at 1.5 Tesla MRI Combined With Semiautomatic Segmentation for Differential Cortical and Medullary Assessment. *Medicine*. 2016; 95:e3083. doi:10.1097/MD.0000000000003083. [PubMed: 26986143]
21. Artz NS, Sadowski EA, Wentland AL, et al. Reproducibility of renal perfusion MR imaging in native and transplanted kidneys using non-contrast arterial spin labeling. *J Magn Reson Imaging*. 2011; 33:1414–21. doi:10.1002/jmri.22552. [PubMed: 21591011]
22. Ritt M, Janka R, Schneider MP, et al. Measurement of kidney perfusion by magnetic resonance imaging: comparison of MRI with arterial spin labeling to para-aminohippuric acid plasma clearance in male subjects with metabolic syndrome. *Nephrol Dial Transplant*. 2010; 25:1126–33. doi:10.1093/ndt/gfp639. [PubMed: 19934080]
23. Artz NS, Wentland AL, Sadowski EA, et al. Comparing kidney perfusion using noncontrast arterial spin labeling MRI and microsphere methods in an interventional swine model. *Invest Radiol*. 2011; 46:124–31. doi:10.1097/RLI.0b013e3181f5e101. [PubMed: 22609830]
24. Heusch P, Wittsack HJ, Blondin D, et al. Functional evaluation of transplanted kidneys using arterial spin labeling MRI. *J Magn Reson Imaging*. 2014; 40:84–9. doi:10.1002/jmri.24336. [PubMed: 24123319]
25. Foundation, NK. KDOQI Clinical Practice Guidelines for Chronic Kidney Disease: Evaluation, Classification, and Stratification. 2002. 2016 [Accessed 8/8/2016]
26. Inci A1 SF, Coban M3, Olmaz R1, Dolu S1, Sankaya M1, Yılmaz N4. Soluble Klotho and fibroblast growth factor 23 levels in diabetic nephropathy with different stages of albuminuria. *J Investig Med*. 2016; 64:1128–33. doi:10.1136/jim-2016-000142.
27. Shimizu K, Kosaka N, Fujiwara Y, et al. Arterial Transit Time-corrected Renal Blood Flow Measurement with Pulsed Continuous Arterial Spin Labeling MR Imaging. *Magnetic resonance in*

- medical sciences : MRMS : an official journal of Japan Society of Magnetic Resonance in Medicine. 2016 doi:10.2463/mrms.mp.2015-0117.
28. Krolewski AS. Progressive renal decline: the new paradigm of diabetic nephropathy in type 1 diabetes. *Diabetes Care*. 2015; 38:954–62. doi:10.2337/dc15-0184. [PubMed: 25998286]
  29. Levey AS, Stevens LA, Schmid CH, et al. A new equation to estimate glomerular filtration rate. *Annals of internal medicine*. 2009; 150:604–12. [PubMed: 19414839]
  30. Ordidge RJ, Wylezinska M, Hugg JW, et al. Frequency offset corrected inversion (FOCI) pulses for use in localized spectroscopy. *Magn Reson Med*. 1996; 36:562–6. [PubMed: 8892208]
  31. Jenkinson M, Bannister P, Brady M, et al. Improved optimization for the robust and accurate linear registration and motion correction of brain images. *NeuroImage*. 2002; 17:825–41. [PubMed: 12377157]
  32. Wu WC, Su MY, Chang CC, et al. Renal perfusion 3-T MR imaging: a comparative study of arterial spin labeling and dynamic contrast-enhanced techniques. *Radiology*. 2011; 261:845–53. doi:10.1148/radiol.11110668. [PubMed: 22095996]
  33. Karger N, Biederer J, Lusse S, et al. Quantitation of renal perfusion using arterial spin labeling with FAIR-UFLARE. *Magn Reson Imaging*. 2000; 18:641–7. doi:S0730725X00001557 [pii]. [PubMed: 10930773]
  34. de Bazelaire CM, Duhamel GD, Rofsky NM, et al. MR imaging relaxation times of abdominal and pelvic tissues measured in vivo at 3.0 T: preliminary results. *Radiology*. 2004; 230:652–9. doi: 10.1148/radiol.2303021331. [PubMed: 14990831]
  35. Foundation, PS. Python. 2016. 2016
  36. Stéfan van der Walt, SCCaGV. The NumPy Array: A Structure for Efficient Numerical Computation. *Computing in Science & Engineering*. 2011; 13:22–30.
  37. Sullivan GM, Feinn R. Using Effect Size-or Why the P Value Is Not Enough. *Journal of graduate medical education*. 2012; 4:279–82. doi:10.4300/JGME-D-12-00156.1. [PubMed: 23997866]

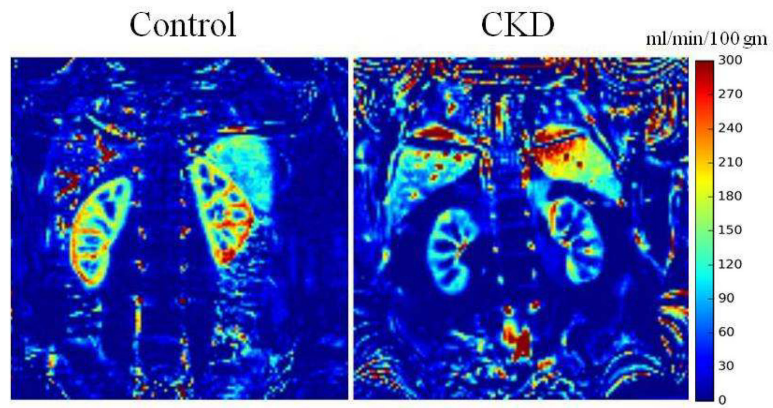


**Figure 1.**

Representative images obtained with retrospective 2D navigator gated ASL sequence. On the left is the ASL perfusion map from a healthy control and on the right is one from a subject with CKD. The window and level settings were the same for both. Note the reduced blood flow in the subject with CKD compared to control.

**Table 1-1**

Information of gender, race and medicine

	<b>N</b>	<b>Male: Female</b>	<b>Race (AA:C:O)</b>	<b>Medications</b>
<b>CKD</b>	33	18:15	11:22:0	ACEi/ARBs (n=23)
<b>Control</b>	30	6:24	10:16:4	n/a

Note: AA=African American; C=Caucasian; O=Others

Author Manuscript

Author Manuscript

Author Manuscript

Author Manuscript

**Table 1-2**

Interquartile range of age, BMI, eGFR and urine protein

Parameter	Group	N	Mean	SD	Median	Q1 (25%)	Q3 (75%)
Age	CKD	33	68.1	9.0	69.4	61.0	74.8
	Control	30	42.0	18.1	42.7	22.5	55.0
BMI (kg/m <sup>2</sup> )	CKD	33	31.8	6.3	30.1	27.3	35.8
	Control	30	24.5	3.3	23.3	22.8	26.4
eGFR (ml/min/1.73m <sup>2</sup> )	CKD	33	50.0	13.9	46.7	39.3	62.9
	Control	30	100.7	17.7	101.9	87.0	111.6
Urine protein (g)	CKD	28	1.86	4.6	0.175	0	1.045
	Control	n/a	n/a	n/a	n/a	n/a	n/a

Note: n/a=not available

**Table 2**

Summary for variables between CKD and Control at baseline

<i>Parameter</i>	<i>Health Status</i>	<i>n</i>	<i>Mean</i>	<i>SD</i>	<i>P value</i>	<i>d value</i>
<i>Age</i>	CKD	33	68.1	9.0	<0.001	<b>1.83</b>
	healthy	30	42.0	18.1		
<i>BMI</i>	CKD	33	31.7	6.3	<0.001	<b>1.4</b>
	healthy	30	24.5	3.3		
<i>eGFR</i>	CKD	33	50.0	13.9	<0.001	<b>3.19</b>
	healthy	30	100.7	17.7		
<i>Cor_BF</i>	CKD	33	108.4	36.4	<0.001	<b>2.52</b>
	healthy	30	207.3	41.8		
<i>Med_BF</i>	CKD	33	23.2	8.9	<0.001	<b>1.5</b>
	healthy	26	42.6	15.8		

**Table 3**Summary of Spearman Correlation Coefficients ( $\rho$ )

	<b>age</b>	<b>eGFR</b>	<b>Cor_BF</b>	<b>Med_BF</b>	<b>BMI</b>
<i>age</i>	1	-0.62	-0.58	-0.39	0.47
<i>p value</i>		<b>&lt;.0001</b>	<b>&lt;.0001</b>	<b>0.0028</b>	<b>&lt;.0001</b>
<i>eGFR</i>		1	0.67	0.62	-0.58
<i>p value</i>			<b>&lt;.0001</b>	<b>&lt;.0001</b>	<b>&lt;.0001</b>
<i>Cor_BF</i>			1	0.70	-0.55
<i>p value</i>				<b>&lt;.0001</b>	<b>&lt;.0001</b>
<i>Med_BF</i>				1	-0.38
<i>p value</i>					<b>0.0029</b>
<i>BMI</i>					1

Author Manuscript

Author Manuscript

Author Manuscript

Author Manuscript

**Table 4-1**

Multiple linear regression analysis with eGFR as independent and BF as dependent variable

Region	Parameter	Estimate	SE	P value
<i>Cor BF</i>	Intercept	54.70	14.61	<b>0.0004</b>
	Slope (eGFR)	1.33	0.18	<b>&lt;0.0001</b>
<i>Med BF</i>	Intercept	10.42	3.87	<b>0.0092</b>
	Slope (eGFR)	0.28	0.05	<b>&lt;0.0001</b>

Author Manuscript

Author Manuscript

Author Manuscript

Author Manuscript



**Table 4-2**

Multiple linear regression analysis with eGFR as independent and BF as dependent variable with adjustment for age and BMI

Region	Parameter	Estimate	SE	P value
<i>Cor BF</i>	Intercept	143.49	50.01	<b>0.0057</b>
	Slope (eGFR)	0.99	0.26	<b>0.0004</b>
	Slope (age)	-0.38	0.39	<b>0.345</b>
	Slope (BMI)	-1.50	1.04	<b>0.1561</b>
<i>Med BF</i>	Intercept	15.11	13.50	<b>0.2682</b>
	Slope (eGFR)	0.27	0.07	<b>0.0004</b>
	Slope (age)	0.02	0.10	<b>0.8469</b>
	Slope (BMI)	-0.18	0.28	<b>0.5307</b>

**Table 5**

Summary of Age- and BMI- Matched Groups

Parameter	Health Status	N	Mean	SD	P value
<i>age</i>	CKD	6	63.22	7.15	0.6884
	healthy	6	65.07	9.86	
<i>BMI</i>	CKD	6	25.89	3.34	0.6408
	healthy	6	25.02	2.93	
<i>egfr</i>	CKD	6	45.73	11.72	<.0001
	healthy	6	92.76	11.36	
<i>Cor_BF</i>	CKD	6	107.4	42.8	<b>0.002</b>
	healthy	6	187.51	20.44	
<i>Med_BF</i>	CKD	6	15.43	8.43	<b>0.0019</b>
	healthy	6	39.18	11.13	